pISSN 2384-1095
eISSN 2384-1109

iMRI 2017;21:65-70

https://doi.org/10.13104/imri.2017.21.2.65

iMRI
Investigative Magnetic Resonance Imaging

Depiction of Acute Stroke Using 3-Tesla Clinical Amide Proton Transfer Imaging: Saturation Time Optimization Using an *in vivo* Rat Stroke Model, and a Preliminary Study in Human

Ji Eun Park[1], Ho Sung Kim[1], Seung Chai Jung[1], Jochen Keupp[2], Ha-Kyu Jeong[3], Sang Joon Kim[1]

[1]Department of Radiology and Research Institute of Radiology, University of Ulsan College of Medicine, Asan Medical Center, Seoul, Korea
[2]Philips Research, Hamburg, Germany
[3]Philips Healthcare Korea, Philips House, Seoul, Korea

Original Article

Received: February 23, 2017
Revised: March 20, 2017
Accepted: March 28, 2017

Correspondence to:
Seung Chai Jung, M.D., Ph.D.
Department of Radiology and Research Institute of Radiology, University of Ulsan College of Medicine, Asan Medical Center, 88 Olympic-ro 43-gil, Songpa-gu, Seoul 05505, Korea.
Tel. +82-2-3010-3949
Fax. +82-2-3010-6645
E-mail: dynamics79@gmail.com

This work was supported by the Advanced MRI in Neuroradiology study group at the Korean Society of Magnetic Resonance in Medicine (KSMRM).
This study was supported by a grant (2016-690) from the Asan Institute for Life Sciences, Asan Medical Center, Seoul, Korea.

Purpose: To optimize the saturation time and maximizing the pH-weighted difference between the normal and ischemic brain regions, on 3-tesla amide proton transfer (APT) imaging using an *in vivo* rat model.
Materials and Methods: Three male Wistar rats underwent middle cerebral artery occlusion, and were examined in a 3-tesla magnetic resonance imaging (MRI) scanner. APT imaging acquisition was performed with 3-dimensional turbo spin-echo imaging, using a 32-channel head coil and 2-channel parallel radiofrequency transmission. An off-resonance radiofrequency pulse was applied with a Sinc-Gauss pulse at a $B_{1,rms}$ amplitude of 1.2 μT using a 2-channel parallel transmission. Saturation times of 3, 4, or 5 s were tested. The APT effect was quantified using the magnetization-transfer-ratio asymmetry at 3.5 ppm with respect to the water resonance (APT-weighted signal), and compared with the normal and ischemic regions. The result was then applied to an acute stroke patient to evaluate feasibility.
Results: Visual detection of ischemic regions was achieved with the 3-, 4-, and 5-s protocols. Among the different saturation times at 1.2 μT power, 4 s showed the maximum difference between the ischemic and normal regions (-0.95%, P = 0.029). The APTw signal difference for 3 and 5 s was -0.9% and -0.7%, respectively. The 4-s saturation time protocol also successfully depicted the pH-weighted differences in an acute stroke patient.
Conclusion: For 3-tesla turbo spin-echo APT imaging, the maximal pH-weighted difference achieved when using the 1.2 μT power, was with the 4 s saturation time. This protocol will be helpful to depict pH-weighted difference in stroke patients in clinical settings.

Keywords: Amide proton transfer; Stroke; pH-difference; Saturation time

INTRODUCTION

pH-weighted imaging has previously shown promise in the depiction of acute stroke (1) since it is able to distinguish tissues with or without metabolic acidosis, before irreversible damage occurs. Amide proton transfer (APT) imaging, a variant of chemical exchange saturation transfer (CEST) imaging, has been experimentally (2) and clinically (3) evaluated in stroke, to depict pH-weighted differences using endogenous contrast of intermediately exchanged amide protons at 3.5 ppm. This new imaging biomarker may have the potential to be incorporated into stroke imaging protocols, since depicting ischemic penumbra remains a challenge using computed tomography or diffusion- or perfusion-weighted magnetic resonance imaging (MRI) (4-6). However, to date, clinical studies have been sparse for APT imaging in stroke (3).

Hurdles for the clinical application of APT imaging include the practical concern of applying a new imaging biomarker in patients with acute stroke, and the technical limitations of achieving sufficient pH-weighted differences between ischemic and unaffected tissue. Tietze et al. (3) addressed the limitations of APT imaging with a 3-dimensional (3D) gradient-echo sequence that counters the effects of B_0 field inhomogeneity and direct water saturation capable of obscuring lesions in the vicinity of the cerebrospinal fluid space. The recent development of the 3D turbo spin-echo (TSE) sequence with 2-channel parallel radiofrequency (RF) transmission (7) may provide more robust motion and artifact correction, compared to the gradient-echo protocol, enabling a sufficiently long saturation time. Using this spin-echo sequence, optimization of off-resonance RF power was tested at 1, 2, and 3 μT with a 500 ms saturation time. However, this saturation time is short and possibly not optimal, as the cumulative pH-weighted effect on the water is maximized when the labeling process is given a sufficiently long saturation time (8).

Since no current literature is available for optimizing the saturation time with TSE APT imaging at 3T for stroke model, we evaluated clinically feasible saturation times, in order to maximize the pH-weighted difference between the normal appearing brain (NAB) and ischemic regions. Unlike a previous phantom study (9), we used an *in vivo* middle cerebral artery occlusion (MCAO) rat model, followed by histopathological staining, to translate the 3T TSE APT sequence into the clinic. The purpose of our study was to optimize the saturation time, thus maximizing the pH-weighted difference between the normal appearing brain and ischemic regions on 3T APT imaging, using an *in vivo* rat model.

MATERIALS AND METHODS

Animal Model

Adult male Wistar rats weighing between 290 to 350 g, were anesthetized (intra-peritoneal chloral hydrate) and immobilized. All animal procedures were approved by our Institutional Animal Care and Use Committee. Permanent MCAO was applied by inserting a 4-0 silk suture coated with a commercialized silicon rubber-coated 5-0 nylon monofilament (tip diameter: 0.35-0.37 mm) into the lumen of the internal carotid artery, to block the origin of the middle cerebral artery. Immediately after completion of the MRI procedure, the rats were sacrificed, and their brains were removed for histological examination. The infarct core was visualized by applying 2, 3, 5-triphenyltetrazolium hydrochloride (TTC) staining. The time interval from MCAO occlusion to MR imaging was 30 minutes.

APT Imaging Acquisition

Theoretical background for APT experiment

For APT imaging, an off-resonance RF pulse was applied with a sinc-Gauss pulse at a $B_{1,rms}$ amplitude of 1.2 μT. Theoretical background for applying a $B_{1,rms}$ amplitude of 1.2 μT was adopted from Sun et al. (9) using interleaved continuous wave- or pulsed- CEST imaging with single-shot spin-echo (SE) echo planar readout investigated APT asymmetry in stroke on 3T. The study showed that the optimal RF power is approximately 1 μT on 3T, which sufficiently labels the exchangeable protons with minimal spillover effects. On the other hand, Zhao et al. (10) showed that a 2 μT amplitude had better APT difference compared to 1 or 3 μT, but the study was based on a duration of 500 ms. We adopted an amplitude of 1.2 μT, in order to maximize the pH-weighted effect using 3T TSE imaging.

In our study, APT imaging was tested using different saturation times (3, 4, and 5 seconds) at 1.2 μT.

APT acquisition in rat model and a patient

APT acquisition was performed in a 3T clinical scanner (Ingenia 3.0 CX, Philips Healthcare, Best, the Netherlands) using a 32-channel head coil and 2-channel parallel RF transmission, Using a 3-dimensional TSE imaging protocol. The two alternating transmission RF channels enabled a long quasi-continuous saturation RF pulse train beyond the

100% duty cycle (7). The off-resonance frequency used for the saturation RF pulse was irradiated at 7 frequency offsets with 9 acquisitions (-2.7, +2.7, -3.5, +3.5 [3 acquisitions at different echo times (TE)], -4.3, +4.3, -1560 ppm). A B0 map for off-resonance corrections was estimated using the data acquired at 3 different TEs (TE = ±0.4 ms), with an iterative filtering and mapping procedure with spatial smoothing (11). This procedure was adapted for the 3-point Dixon method (12), and was available from the current scanner software.

For the rat model, the other imaging parameters were as follows: repetition time (TR), 4500-5500 ms; echo time (TE), 5.5-10 ms; number of signal averages (NSA), 2; matrix, 80 x 80; slice thickness, 5 mm; field of view (FOV), 50 mm; 5 slices. No fat suppression was applied in the rat model. The scan time was approximately 7 minutes 10 seconds (3s protocol), 7 minutes 20 seconds (4s protocol), and 8 minutes 10 seconds (5s protocol), respectively.

Upon approval of our Institutional Review Board with consent forms, APT imaging was obtained in a patient with acute stroke. Imaging parameters were as follows: TR, 5198 ms; TE, 6.5 ms; NSA, 1; matrix, 120 x 102; slice thickness, 5 mm; FOV, 212 x 184 mm; 5 slices. The scan time for the 4 s saturation time with 5 slices was approximately 2 minutes and 30 seconds.

Diffusion-weighted imaging (DWI)

To visualize the infarct core, DWI was acquired with a multi-shot echoplanar imaging (EPI) sequence. DWI was obtained with the following parameters: TR/TE, 2772/94 ms; diffusion gradient encoding, b = 0, 1000 s/mm^2; FOV, 50 mm; slice thickness/gap, 5 mm/2 mm; matrix, 192 × 192; and acquisition time, 7 minutes and 32 seconds.

Data Analysis

Maps of the magnetization transfer (MT) asymmetry MTRasym = (S[-3.5 ppm]-S[+3.5 ppm])/S0 were calculated

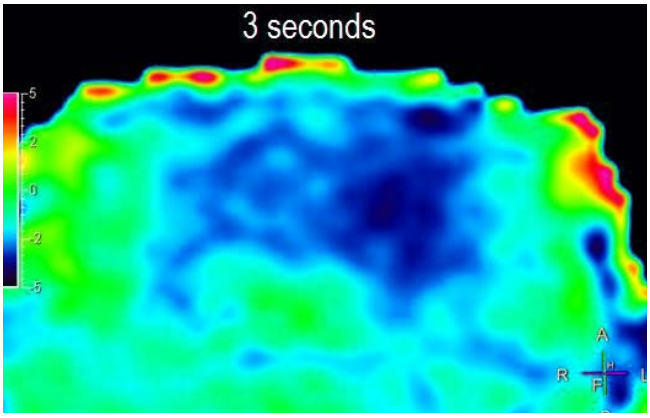

a

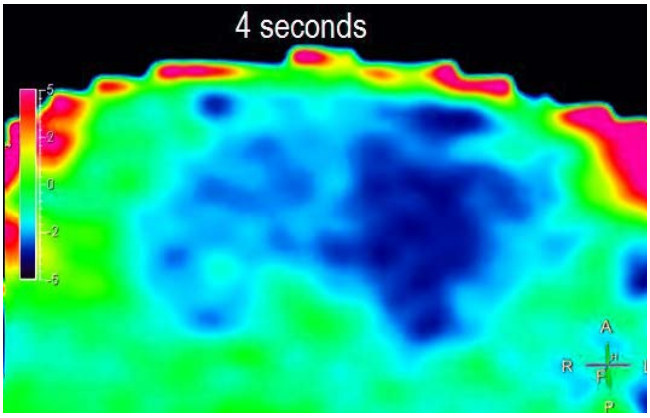

b

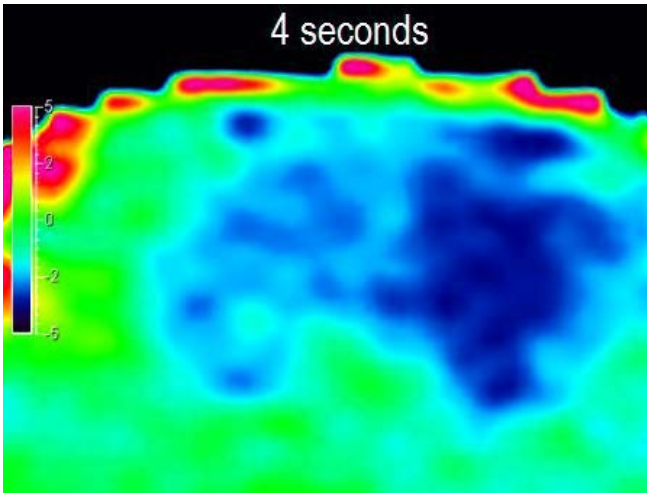

c

Fig. 1. Characterization of acute middle cerebral artery occlusion using amide proton transfer imaging. (a) 3 seconds, (b) 4 seconds, (c) 5 seconds protocol. The 4 s protocol showed maximal visual contrast and localization of the ischemic region.

based on point-by-point interpolation for the δB0 correction (7). Maps of the asymmetric APT ratio were calculated based on the following equation:

APT_{asym}(+3.5 ppm) = MTR(-3.5 ppm) — MTR(+3.5 ppm)

The map was calculated using δB0 point-by-point corrected interpolated images, S[-3.5 ppm] and S[+3.5 ppm]. For APTw signal maps, quality checks and visual assessments were applied by a neuroradiologist (J.E.P., with 5 years of experience) and MR specialist (H.K.J., with 15 years of experience of MR acquisition) in consensus.

Free-hand regions-of-interests (ROIs) were drawn by a neuroradiologist (J.E.P.) at the high signal lesion on DWI on the MR console, using the software incorporated into the MR imaging unit. The same ROI trace was then transferred to the contralateral NAB, and APTw signal was calculated. The APTw signal difference between the ischemic regions and the NAB was calculated and compared among different saturation times. Quantitative analysis was obtained for 5 slices from each rat. The Kruskall-Wallis test was performed to compared the 3,4, and 5 s conditions.

RESULTS

The MCAO model was successfully applied in all 3 Wistar rats, with acceptable quality of APT images in all cases. Figure 1 shows that the APT imaging depicted the ischemic region, and that this changed noticeably between the 3-, 4-, and 5-second conditions.

Table 1 summarizes the quantitative results for the 3-, 4-, and 5-second conditions. The APTw signal difference between the ischemic regions and NAB was maximized in the 4-second protocol. The median APT difference for the 3-, 4-, and 5-second protocols was -1.03%, -1.22%, and -0.82%, respectively. Notably, the APT difference was reduced in the 5-second protocol compared to the 3-second protocol. On Kruskall-Wallis test, the APTw signal difference on the 4-second protocol was significantly larger than the 3- or 5-second protocols (-0.95%, p = 0.029)

DWI and TTC staining showed decreased APTw signal, corresponding to the diffusion restriction region and non-stain regions on TTC staining (Fig. 2).

The protocol was applied to a patient 4 days after

Table 1. APT Difference between Ischemic Regions and Normal Appearing Brain, in a Rat Model, According to RF Saturation Time

Saturation time	APTw signal difference	P-value	Ischemic region	Normal appearing brain
3 seconds	-0.9 (-1.03, -0.9)	0.029	-3.76 (-4.81, -3.45)	-2.73 (-2.77, -2.67)
4 seconds	-0.95 (-1.76, -0.87)		-4.7 (-4.30, -3.33)	-2.51 (-2.86, -2.38)
5 seconds	-0.7 (-0.74, -0.6)		-3.62 (-3.80, -3.50)	-2.8 (-2.90, -2.70)

Numbers in parenthesis are 25 quartile and 75 quartiles, respectively.
APT = amide proton transfer; APTw = APT-weighted; RF = radiofrequency

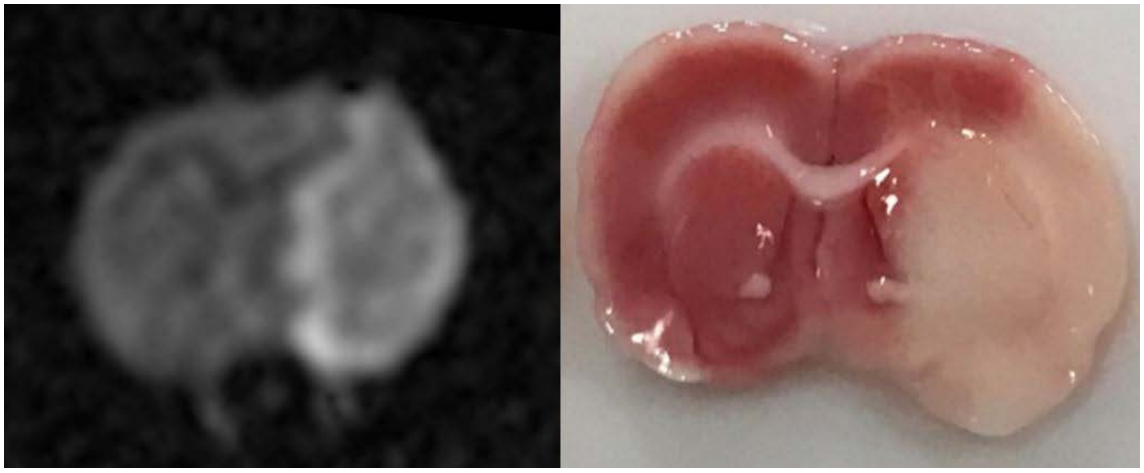

Fig. 2. Diffusion-weighted imaging and TTC (triphenyltetrazolium hydrochloride) stain for the same Wistar rat shown in Figure 1, shows the ischemic region matched with amide proton transfer imaging.

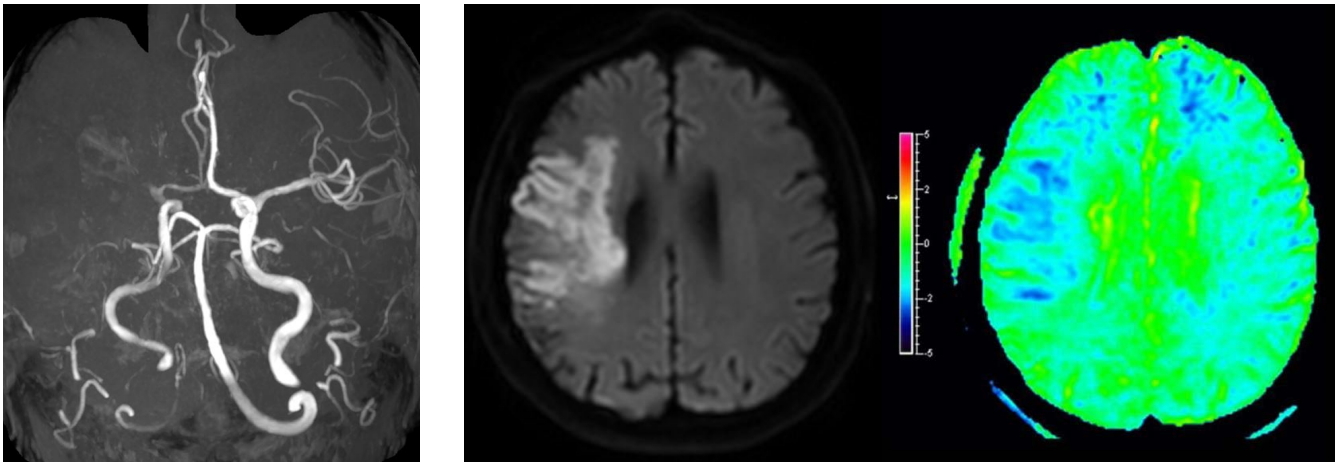

a b

Fig. 3. Amide proton transfer (APT) imaging with a 4 s saturation time protocol applied to a 69-year-old male, 4 days after an acute middle cerebral artery occlusion (a). (b) The diffusion-restriction region matched the reduced APT-weighted signal region, compared to the contralateral normal appearing brain.

a middle cerebral artery infarction, and it successfully depicted APT contrast between the ischemic region and NAB (Fig. 3).

DISCUSSION

Our study utilized APT imaging at 3-T (3T), and we present the difference between ischemic region and normal appearing region in both an *in vivo* rat model and a human case. We adopted the saturation power from a study by Sun et al. (9) on 3T tested different saturation times, ranging from 3 to 5 s, and showed that the maximal APT difference was achieved with a saturation time of 4 s at an amplitude of 1.2 μT. The results of our study support the clinical use of 3T APT imaging with fast multi-slice imaging and an automatic image processing algorithm. The rat brain is considerably smaller than the human brain, but negative contrast in ischemic regions was successfully depicted. In addition, the same saturation time was applied to a patient with acute stroke, and we successfully illustrated the APT contrast within a scan time of 2 minutes and 30 seconds.

Interestingly, a longer saturation time does not correspond to better APT contrast. Saturation times of 3 and 4 s gave better contrast between ischemic regions and the NAB, as compared to 5 s. This may come from a co-existing solid macromolecular MT effect (9, 13) that is more pronounced at a higher RF power, or possible intra- and inter-molecular nuclear Overhauser effects (10). Similar results were obtained by Sun et al. (9), who showed that the optimal saturation power is achieved at around 1 μT, and APT contrast decreased at higher power fields. Since clinical scanners have specific absorption rate limitations, low power levels will be more beneficial than higher power levels. On the other hand, a longer saturation time is beneficial for the cumulative effect on water, which gets maximized when the labeling process is given with a sufficiently long saturation time (8).

The use of APT imaging has been suggested to help stroke depiction by subdividing the perfusion-diffusion mismatched region into regions with and without tissue acidosis (1, 2). Diffusion restricted regions often represent an ischemic core, but they can sometimes recover (14), and perfusion-weighted imaging also includes regions with benign oligemia. A pH-sensitive MR imaging may depict metabolic heterogeneity within homogenously-looking diffusion restriction areas. Previous studies found that average pH-weighted imaging deficits were always equal to or larger than the diffusion restricted regions, but smaller than the perfusion deficits (15, 16). The pH-weighted imaging depicts regions with impaired metabolism that are still reversible (15). It has the potential to differentiate areas with "infarction" from those of "salvageable tissue" using mismatch areas between diffusion-weighted imaging and pH-weighted imaging. Thus, APT imaging is expected to more precisely delineate tissue-at-risk regions, in which both a pH (reduced APT regions) and perfusion decrease has occurred, and subsequently guide patients on further

intervention therapy.

The main limitation of our study is that it was conducted on a small number of subjects. Moreover, APT imaging can be affected by other signal contributors of broad macromolecular magnetization and spin-lattice relaxation (13, 17, 18); thus, the signal source of APT imaging in stroke needs to be further investigated. However, our study has successfully demonstrated APT contrast in an *in vivo* rat model using a 3 T protocol and 32-channel head coil that can translate immediately into the clinic.

In conclusion, the maximal pH-weighted difference was achieved with a 4 s saturation time when using a 1.2 μT power level with 3T TSE APT imaging. The protocol was successfully applied to a stroke patient, and will be helpful to depict pH-weighted difference in stroke patients in the clinic.

REFERENCES

1. Zhou J, van Zijl PC. Defining an acidosis-based ischemic penumbra from pH-weighted MRI. Transl Stroke Res 2011;3:76-83
2. Sun PZ, Benner T, Copen WA, Sorensen AG. Early experience of translating pH-weighted MRI to image human subjects at 3 Tesla. Stroke 2010;41:S147-151
3. Tietze A, Blicher J, Mikkelsen IK, et al. Assessment of ischemic penumbra in patients with hyperacute stroke using amide proton transfer (APT) chemical exchange saturation transfer (CEST) MRI. NMR Biomed 2014;27:163-174
4. Campbell BC, Mitchell PJ, Kleinig TJ, et al. Endovascular therapy for ischemic stroke with perfusion-imaging selection. N Engl J Med 2015;372:1009-1018
5. Kidwell CS, Jahan R, Gornbein J, et al. A trial of imaging selection and endovascular treatment for ischemic stroke. N Engl J Med 2013;368:914-923
6. Meng X, Fisher M, Shen Q, Sotak CH, Duong TQ. Characterizing the diffusion/perfusion mismatch in experimental focal cerebral ischemia. Ann Neurol 2004;55:207-212
7. Keupp J, Baltes C, Harvey PR, van den Brink J. Parallel RF transmission based MRI technique for highly sensitive detection of amide proton transfer in the human brain at 3T. Proc Intl Soc Mag Reson Med 2011;19:710
8. Zhu H, Jones CK, van Zijl PC, Barker PB, Zhou J. Fast 3D chemical exchange saturation transfer (CEST) imaging of the human brain. Magn Reson Med 2010;64:638-644
9. Sun PZ, Benner T, Kumar A, Sorensen AG. Investigation of optimizing and translating pH-sensitive pulsed-chemical exchange saturation transfer (CEST) imaging to a 3T clinical scanner. Magn Reson Med 2008;60:834-841
10. Zhao X, Wen Z, Huang F, et al. Saturation power dependence of amide proton transfer image contrasts in human brain tumors and strokes at 3 T. Magn Reson Med 2011;66:1033-1041
11. Xiang QS. Two-point water-fat imaging with partially-opposed-phase (POP) acquisition: an asymmetric Dixon method. Magn Reson Med 2006;56:572-584
12. Eggers H, Brendel B, Duijndam A, Herigault G. Dual-echo Dixon imaging with flexible choice of echo times. Magn Reson Med 2011;65:96-107
13. Scheidegger R, Wong ET, Alsop DC. Contributors to contrast between glioma and brain tissue in chemical exchange saturation transfer sensitive imaging at 3 Tesla. Neuroimage 2014;99:256-268
14. Kidwell CS, Alger JR, Saver JL. Evolving paradigms in neuroimaging of the ischemic penumbra. Stroke 2004;35:2662-2665
15. Sun PZ, Zhou J, Sun W, Huang J, van Zijl PC. Detection of the ischemic penumbra using pH-weighted MRI. J Cereb Blood Flow Metab 2007;27:1129-1136
16. Sun PZ, Cheung JS, Wang E, Lo EH. Association between pH-weighted endogenous amide proton chemical exchange saturation transfer MRI and tissue lactic acidosis during acute ischemic stroke. J Cereb Blood Flow Metab 2011;31:1743-1750
17. Heo HY, Zhang Y, Lee DH, Hong X, Zhou J. Quantitative assessment of amide proton transfer (APT) and nuclear overhauser enhancement (NOE) imaging with extrapolated semi-solid magnetization transfer reference (EMR) signals: Application to a rat glioma model at 4.7 Tesla. Magn Reson Med 2016;75:137-149
18. Li H, Li K, Zhang XY, et al. R1 correction in amide proton transfer imaging: indication of the influence of transcytolemmal water exchange on CEST measurements. NMR Biomed 2015;28:1655-1662